DOI: 10.2478/auom-2025-0018
An. Şt. Univ. Ovidius Constanţa **Vol. 33(2),2025, 45–65**

Numerical solution of nonlinear reaction advection-diffusion equation using the modified collocation method

E-M. Craciun, S.K. Tiwari, S. Das

Abstract

This article presents a numerical solution of the nonlinear reaction-advection-diffusion equation with specified initial and boundary conditions using a modified cubic B-spline collocation method. Nonlinear terms are linearised using the Crank-Nicholson method. The derived numerical scheme is shown to be unconditionally convergent through stability analysis. The accuracy of the numerical scheme has been verified by its application to the three standard instances. The numerical findings are then compared with the existing analytical results by employing the l^2 and l^∞ error norms. The main feature of this article is the graphical presentation of the numerical solution of the concerned model for different sets of advection, diffusion and reaction coefficients to show the effect on the solute profile when advection and diffusion terms are both nonlinear. Nonlinear reaction-advection-diffusion equations have found applications in diverse areas like groundwater and water pollution studies.

1 Introduction

In science and technology, the fluid flow through porous media has enormous theoretical and practical implications. Any true porous material is made up of a combination of particles that have been weathered from rock or the remnants of extinct animals. A system of variously sized particles makes up a porous

Key Words: Collocation method, Cubic B-spline, Crank-Nicholson method
Received: 11.11.2024
Accepted: 15.03.2025

medium rather than a compact substance. There are applications in oil exploration, environmental problems, geophysical problems, and industrial problems, such as the movement of liquid and gas through soil and rock (e.g., shell oil extraction), clay, gravel, and sand, or sponges and foam [1, 2, 3, 4, 5]. Two primary categories can be distinguished between groundwater flows across the saturated zone: those with a phreatic (free) surface and those with a confined surface. The governing equations for these groups are completely different. The free flow has a nonlinear governing equation and a linear one for the flow with a constrained surface. Different nonlinear systems for various natural phenomena can be modelled using nonlinear partial differential equations. The first nonlinear diffusion was identified in plasma physics by Berryman and Holland [19]. Using the Buckingham-Darcy law [29, 30] and the equation of continuity for one-dimensional vertical flow

$$\frac{\partial u}{\partial t} = -\frac{\partial q}{\partial x},$$
$$\text{and} \quad q = -D(u)\frac{\partial u}{\partial x} - K(u),$$

respectively, Kovarik [31] derived the equation governing groundwater flow with a confined surface as

$$\frac{\partial u}{\partial t} = \frac{\partial}{\partial x}\left(D(u)\frac{\partial u}{\partial x}\right) - \frac{dK}{du}\frac{\partial u}{\partial x},$$

where q is flux density, u is volumetric water content, x is depth below the soil surface, $D(u)$ is the concentration-dependent soil water diffusivity and $K(u)$ is the concentration-dependent hydraulic conductivity. The above equation describes the flow in porous media, diffusion in semiconductors, and other nonlinear processes. For soil moisture flow, $0 \leq u \leq 1$, where a saturated medium corresponds to $u = 1$, whereas a dry medium corresponds to $u = 0$. For $D(u) = u$ and $K(u) = -\nu u^2$, the above equation becomes

$$u_t = uu_{xx} + u_x^2 + 2\nu uu_x, \tag{1}$$

where ν is a physical parameter of the inclination of the bed associated with the movement of buoyancy-driven plumes in inclined porous media.
The creation and consumption of molecules can occur within an element of space during a reaction. The diffusion equation is supplemented with these events, resulting in the reaction-diffusion equation that takes the following form:

$$\frac{\partial u}{\partial t} = D\nabla^2 u + R(u,t),$$

where $R(u,t)$ denotes reaction term at time t. The following nonlinear reaction advection-diffusion equation (nonlinear RADE) will be discussed in this article.

$$\frac{\partial u}{\partial t} = D\frac{\partial}{\partial x}\left(u\frac{\partial u}{\partial x}\right) - \nu u\frac{\partial u}{\partial x} - \lambda u(1-u), \qquad D > 0, \nu, \lambda \in \mathbb{R} \tag{2}$$

under the prescribed initial and boundary conditions given by

$$u(x,0) = f_1(x), \tag{3}$$

$$u(r,t) = f_2(t), \tag{4}$$

$$u(s,t) = f_3(t), \quad \text{where } r, s \in \mathbb{R}. \tag{5}$$

There are only a few simple cases for which an analytical solution is available. Therefore, the development of accurate and efficient numerical methods is extremely important to solve the nonlinear RADE. Many researchers have developed different numerical methods to study different nonlinear diffusion-advection equations. After studying the asymptotic solution of equation (1), Loubens and Ramakrishnan [11] have demonstrated that, for compactly supported beginning data, the solution is characterized by two moving boundaries propagating at a limited speed across an $O(\sqrt{t})$ distance. Furthermore, it was demonstrated in [12] that the interface shape evolution of a gravity tongue propagating up an inclined layer with respect to a moving frame is governed by equation (1). Using the functional constraint method, Polyanin and Zhurov [13] have found some solutions to nonlinear delay reaction-diffusion equations. Lu et al. [15] generalised the BurgersFisher equation using the first integral method and obtained some exact solutions. Jaiswal et al. [17] used the operational matrix method to study the nonlinear partial differential equation for porous media.

An advantageous gene's propagation across a population was first studied using the reaction-diffusion equation, a one-dimensional parabolic nonlinear partial differential equation provided by R.A. Fisher[7]. Kenkre[8] studied the dynamics of bacteria, the formation of patterns, and the propagation of epidemics using data from variations of the Fisher equation. The branching Brownian motion process [10] was analysed using the Fisher equation. In the Fisher equation with degenerate nonlinear diffusion, non-sharp travelling wavefronts were examined by Sherratt and Marchant[14]. Mittal and Arora [16] solved the Fisher equation numerically by developing an efficient B-spline scheme. The nonlinear diffusion problem was numerically solved by Dwivedi and Das[18] utilising Fibonacci collocation and non-standard/standard finite difference techniques. Kumar and Arora [24] studied the solution of the Fisher-Kolmogorov-Petrovsky equation using the Haar scale-3 wavelet collocation method. Many authors used B-spline functions to develop numerical methods

[20, 23, 22, 25] for solving different diffusion Fisher equations. The piecewise continuous nature of spline functions, specifically B-spline functions, makes them very useful for approximating numerical solutions to partial differential equations.
The remaining article is organised as follows. With the help of the definition and properties of cubic B-splines, mathematical derivation and implementation of the method are covered in sections 2 and 3. Stability analysis is being done in section 4. To show the accuracy of the numerical scheme, three particular cases of the proposed model are solved numerically in section 5. The numerical solution of the proposed mathematical model using a numerical technique developed for the specified initial and boundary conditions is shown in section 6. Section 7 summarises the overall work.

2 Description of the numerical scheme

Let the domain be $[r, s]$ and $r = x_0 < x_1 < x_2 < ..... < x_{M-1} < x_M = s$ be a uniform partition in $M + 1$ node points such that $x_{i+1} - x_i = h$ is the length of each sub-interval.
For the proposed model (2), an approximate solution $f(x, t) \approx u(x, t)$ can be expressed in the following form using the cubic B-spline collocation method as

$$f(x,t) = \sum_{j=1}^{n} \alpha_j(t) B_j(x), \tag{6}$$

where $B_j(x)$'s are the basis functions of B-splines and $\alpha_j(t)$'s are the time-dependent constants to be determined by applying initial and boundary conditions and using the collocation method.
The cubic B-spline basis function $B_j(x)$ at any knot point is defined as

$$B_j(x) = \frac{1}{h^3} \begin{cases} (x - x_{j-2})^3, & x \in [x_{j-2}, x_{j-1}) \\ (x - x_{j-2})^3 - 4(x - x_{j-1})^3, & x \in [x_{j-1}, x_j) \\ (x_{j+2} - x)^3 - 4(x_{j-1} - x)^3, & x \in [x_j, x_{j+1}) \\ (x_{j+2} - x)^3, & x \in [x_{j+1}, x_{j+2}) \\ 0, & \text{otherwise,} \end{cases} \tag{7}$$

where $\{B_{-1}, B_0, B_1, B_2, ..., B_{M-1}, B_M, B_{M+1}\}$ forms a basis set for the cubic B-spline functions for the considered domain.
From Table 1, we can get values of basis functions and their derivatives at each knot point.

Let us denote $(x_i, t) = (\xi_i)$ for further calculations.
Using the method of finite difference and Taylor expansion, the first and

Table 1: Coefficients of cubic B-splines and its derivatives at knot x_j

x	x_{j-2}	x_{j-1}	x_j	x_{j+1}	x_{j+2}
$B_j(x)$	0	1	4	1	0
$B_j'(x)$	0	$\frac{3}{h}$	0	$\frac{-3}{h}$	
$B_j''(x)$	0	$\frac{6}{h^2}$	$\frac{-12}{h^2}$	$\frac{6}{h^2}$	0

second-order derivatives of the function $f(x_i,t) = f(\xi_i)$ are defined as

$$f'(\xi_i) = u'(\xi_i) + O(h^4), \qquad 0 \le i \le M, \tag{8}$$

$$f''(\xi_i) = u''(\xi_i) - \frac{1}{12}h^2 u^{(4)}(\xi_i) + O(h^4), \qquad i = 0, M. \tag{9}$$

Using the smoothness of the solution $u(x,t)$, and that $f(x,t)$ is a unique cubic spline approximation satisfying prescribed boundary conditions, we have [6] for $i = 0$

$$u^{(4)}(\xi_0) = \frac{2f''(\xi_0) - 5f''(\xi_1) + 4f''(\xi_2) - f''(\xi_3)}{h^2} + O(h^2), \tag{10}$$

for $1 \le i \le M-1$

$$u^{(4)}(\xi_i) = \frac{f''(\xi_{i-1}) - 2f''(\xi_i) + f''(\xi_{i+1})}{h^2} + O(h^2), \tag{11}$$

for $i = M$

$$u^{(4)}(\xi_M) = \frac{2f''(\xi_M) - 5f''(\xi_{M-1}) + 4f''(\xi_{M-2}) - f''(\xi_{M-3})}{h^2} + O(h^2). \tag{12}$$

Using equations (10), (11) and (12) along with approximation (6) in the equations (8) and (9), we get
for $i = 0$

$$u''(x_0) = \sum_{j=-1}^{M+1} \alpha_j(t) \frac{14B_j''(x_0) - 5B_j''(x_1) + 4B_j''(x_2) - B_j''(x_3)}{12}, \tag{13}$$

for $1 \le i \le M-1$

$$u''(x_i) = \sum_{j=-1}^{M+1} \alpha_j(t) \frac{B_j''(x_{i-1}) + 10B_j''(x_i) + B_j''(x_{i+1})}{12}, \tag{14}$$

for $i = M$

$$u''(x_M) = \sum_{j=-1}^{M+1} \alpha_j(t) \frac{14B_j''(x_M) - 5B_j''(x_{M-1}) + 4B_j''(x_{M-2}) - B_j''(x_{M-3})}{12}. \tag{15}$$

The above equations can further be simplified using (7) as
for $i = 0$

$$u''(x_0, t) = \frac{14\alpha_{-1} - 33\alpha_0 + 28\alpha_1 - 14\alpha_2 + 6\alpha_3 - \alpha_4}{2h^2}, \tag{16}$$

for $1 \leq i \leq M - 1$

$$u''(x_i, t) = \frac{\alpha_{i-2} + 8\alpha_{i-1} - 18\alpha_i + 8\alpha_{i+1} + \alpha_{i+2}}{2h^2}, \tag{17}$$

for $i = M$

$$u''(x_M, t) = \frac{14\alpha_{M+1} - 33\alpha_M + 28\alpha_{M-1} - 14\alpha_{M-2} + 6\alpha_{M-3} - \alpha_{M-4}}{2h^2}. \tag{18}$$

Now, the approximations for $u(x,t), u'(x,t)$ and $u''(x,t)$ are used to solve our proposed model numerically. We can discretise the equation (2) using the Crank-Nicholson method as

$$\begin{aligned} \frac{u_i^{n+1} - u_i^n}{\Delta t} &= D\frac{(uu_{xx})_i^{n+1} + (uu_{xx})_i^n}{2} + D\frac{(u_x^2)_i^{n+1} + (u_x^2)_i^n}{2} \\ &- \nu\frac{(uu_x)_i^{n+1} + (uu_x)_i^n}{2} - \lambda\frac{(u(1-u))_i^{n+1} + (u(1-u))_i^n}{2}. \end{aligned} \tag{19}$$

Nonlinear terms are linearised using the Taylor expansion method as

$$\begin{aligned} (uu_{xx})_i^{n+1} &= u_i^{n+1}(u_{xx})_i^n + u_i^n(u_{xx})_i^{n+1} - u_i^n(u_{xx})_i^n, \\ (uu_x)_i^{n+1} &= u_i^{n+1}(u_x)_i^n + u_i^n(u_x)_i^{n+1} - u_i^n(u_x)_i^n, \\ (u_x^2)_i^{n+1} &= 2(u_x)_i^n(u_x)_i^{n+1} - (u_x^2)_i^n, \\ (u^2)_i^{n+1} &= 2(u)_i^n(u)_i^{n+1} - (u^2)_i^n. \end{aligned}$$

Separating the different time level terms of equation (19), we get

$$\begin{aligned} & u_i^{n+1}\left(1 - \frac{D\Delta t}{2}(u_{xx})_i^n + \frac{\nu\Delta t}{2}(u_x)_i^n + \frac{\lambda\Delta t}{2} - \lambda\Delta t u_i^n\right) - \left(\frac{D\Delta t}{2}u_i^n\right)(u_{xx})_i^{n+1} \\ & - \left(D\Delta t(u_x)_i^n - \frac{\nu\Delta t}{2}\right)(u_x)_i^{n+1} = u_i^n\left(1 - \frac{\lambda\Delta t}{2}\right). \end{aligned} \tag{20}$$

Consider

$$U_i = \left(1 - \frac{D\Delta t}{2}(u_{xx})_i^n + \frac{\nu\Delta t}{2}(u_x)_i^n + \frac{\lambda\Delta t}{2} - \lambda\Delta t u_i^n\right),\ V_i = \left(\frac{D\Delta t}{4h^2}u_0^n\right),$$

$$W_i = \frac{3\Delta t}{h}\left(D(u_x)_0^n - \frac{\nu}{2}\right), \gamma_i = \left(1 - \frac{\lambda\Delta t}{2}\right).$$

Using the approximations defined in Section 2, the equation (20) can be simplified as
for $i = 0$

$$\begin{aligned}&(\alpha_{-1}^{n+1} + 4\alpha_0^{n+1} + \alpha_1^{n+1})\left(1 - \frac{D\Delta t}{2}(u_{xx})_0^n + \frac{\nu\Delta t}{2}(u_x)_0^n + \frac{\lambda\Delta t}{2} - \lambda\Delta t u_0^n\right)\\ &- \left(\frac{D\Delta t}{4h^2}u_0^n\right)(14\alpha_{-1}^{n+1} - 33\alpha_0^{n+1} + 28\alpha_1^{n+1} - 14\alpha_2^{n+1} + 6\alpha_3^{n+1} - \alpha_4^{n+1})\\ &- \frac{3\Delta t}{h}\left(D(u_x)_0^n - \frac{\nu}{2}\right)(\alpha_1^{n+1} - \alpha_{-1}^{n+1}) = u_0^n\left(1 - \frac{\lambda\Delta t}{2}\right),\end{aligned} \tag{21}$$

$$\begin{aligned}\implies (U_0 - 14V_0 + W_0)\alpha_{-1}^{n+1} + (4U_0 + 33V_0)\alpha_0^{n+1} + (U_0 - 28V_0 - W_0)\alpha_1^{n+1}\\ + 14V_0\alpha_2^{n+1} - 6V_0\alpha_3^{n+1} + V_0\alpha_4^{n+1} = \gamma_0^n.\end{aligned} \tag{22}$$

Equation (22) can be written as

$$\omega_{01}\alpha_{-1}^{n+1} + \omega_{02}\alpha_0^{n+1} + \omega_{03}\alpha_1^{n+1} + \omega_{04}\alpha_2^{n+1} + \omega_{05}\alpha_3^{n+1} + \omega_{06}\alpha_4^{n+1} = \gamma_0^n, \tag{23}$$

where ω_{0i}'s are coefficients of α_{i-2} in equation (23) respectively.
For $1 \le i \le M-1$

$$\begin{aligned}&(\alpha_{i-1}^{n+1} + 4\alpha_i^{n+1} + \alpha_{i+1}^{n+1})\left(1 - \frac{D\Delta t}{2}(u_{xx})_i^n + \frac{\nu\Delta t}{2}(u_x)_i^n + \frac{\lambda\Delta t}{2} - \lambda\Delta t u_i^n\right)\\ &- \left(\frac{D\Delta t}{4h^2}u_i^n\right)(\alpha_{i-2}^{n+1} + 8\alpha_{i-1}^{n+1} - 18\alpha_i^{n+1} + 8\alpha_{i+1}^{n+1} + \alpha_{i+2}^{n+1}) - \frac{3\Delta t}{h}\\ &\left(D(u_x)_i^n - \frac{\nu}{2}\right)(\alpha_{i+1}^{n+1} - \alpha_{i-1}^{n+1}) = u_i^n\left(1 - \frac{\lambda\Delta t}{2}\right),\end{aligned} \tag{24}$$

$$\begin{aligned}\implies (-V_i)\alpha_{i-2}^{n+1} + (U_i - 8V_i + W_i)\alpha_{i-1}^{n+1} + (4U_i + 18V_i)\alpha_i^{n+1}\\ + (U_i - 8V_i - W_i)\alpha_{i+1}^{n+1} + (-V_i)\alpha_{i+2}^{n+1} = r_i^n.\end{aligned} \tag{25}$$

Equation (25) can be written as

$$\omega_{i1}\alpha_{i-2}^{n+1} + \omega_{i2}\alpha_{i-1}^{n+1} + \omega_{i3}\alpha_i^{n+1} + \omega_{i4}\alpha_{i+1}^{n+1} + \omega_{i5}\alpha_{i+2}^{n+1} = \gamma_i^n. \tag{26}$$

where ω_{ij}'s are coefficients of α_{i+j-3} in equation (26).
For $i = M$

$$
\begin{aligned}
&(\alpha_{M-1}^{n+1} + 4\alpha_M^{n+1} + \alpha_{M+1}^{n+1})\left(1 - \frac{D\Delta t}{2}(u_{xx})_M^n + \frac{\nu\Delta t}{2}(u_x)_M^n + \frac{\lambda\Delta t}{2} - \lambda\Delta t u_M^n\right) \\
&- \left(\frac{D\Delta t}{4h^2}u_M^n\right)(14\alpha_{M+1}^{n+1} - 33\alpha_M^{n+1} + 28\alpha_{M-1}^{n+1} - 14\alpha_{M-2}^{n+1} + 6\alpha_{M-3}^{n+1} - \alpha_{M-4}^{n+1}) \\
&- \frac{3\Delta t}{h}\left(D(u_x)_M^n - \frac{\nu}{2}\right)(\alpha_{M+1}^{n+1} - \alpha_{M-1}^{n+1}) = u_M^n\left(1 - \frac{\lambda\Delta t}{2}\right) \qquad (27)
\end{aligned}
$$

$$
\begin{aligned}
\Longrightarrow V_M\alpha_{M-4}^{n+1} - 6V_M\alpha_{M-3}^{n+1} + 14V_M\alpha_{M-2}^{n+1} + (U_M - 28V_M + W_M)\alpha_{M-1}^{n+1} \\
+ (4U_M + 33V_M)\alpha_M^{n+1} + (U_M - 14V_M - W_M)\alpha_{M+1}^{n+1} = r_M^n. \qquad (28)
\end{aligned}
$$

Equation (28) can be written as

$$
\begin{aligned}
\omega_{M1}\alpha_{M-4}^{n+1} + \omega_{M2}\alpha_{M-3}^{n+1} + \omega_{M3}\alpha_{M-2}^{n+1} + \omega_{M4}\alpha_{M-1}^{n+1} + \omega_{M5}\alpha_M^{n+1} + \omega_{M6}\alpha_{M+1}^{n+1} \\
= \gamma_M^n. \qquad (29)
\end{aligned}
$$

where ω_{Mj}'s are coefficients of α_{M+j-5} in equation (29).
Now, applying the model's specified boundary conditions, we get

$$(\alpha_{-1}^{n+1} + 4\alpha_0^{n+1} + \alpha_1^{n+1}) = f_2[(n+1)\Delta t], \qquad (30)$$

$$(\alpha_{M-1}^{n+1} + 4\alpha_M^{n+1} + \alpha_{M+1}^{n+1}) = f_3[(n+1)\Delta t]. \qquad (31)$$

Considering the above two equations with equations (23), (26) and (29), we have a matrix of order $(M+3) \times (M+3)$ defined as

$$\Omega^{n+1}C^{n+1} = \Gamma^n, \qquad (32)$$

where $\Omega^{n+1} =$

$$
\begin{pmatrix}
1 & 4 & 1 & 0 & 0 & 0 & 0 & \cdots & 0 \\
\omega_{01} & \omega_{02} & \omega_{03} & \omega_{04} & \omega_{05} & \omega_{06} & 0 & \cdots & 0 \\
\omega_{11} & \omega_{12} & \omega_{13} & \omega_{14} & \omega_{15} & 0 & 0 & \cdots & 0 \\
0 & \omega_{21} & \omega_{22} & \omega_{23} & \omega_{24} & \omega_{25} & 0 & \cdots & 0 \\
\vdots & \vdots & \vdots & \vdots & \vdots & \vdots & \vdots & \ddots & \vdots \\
\vdots & \vdots & \vdots & \vdots & \vdots & \vdots & \vdots & \ddots & \vdots \\
0 & \cdots & \cdots & 0 & \omega_{M-11} & \omega_{M-12} & \omega_{M-13} & \omega_{M-14} & \omega_{M-15} \\
0 & \cdots & \cdots & \omega_{M1} & \omega_{M2} & \omega_{M3} & \omega_{M4} & \omega_{M5} & \omega_{M6} \\
0 & \cdots & 0 & 0 & 0 & 0 & 1 & 4 & 1
\end{pmatrix}
$$

$$C^{n+1} = (\alpha_{-1}^{n+1}, \alpha_0^{n+1}, \alpha_1^{n+1}, ..., \alpha_{M-1}^{n+1}, \alpha_M^{n+1}, \alpha_{M+1}^{n+1})^T$$

and

$$\Gamma^n = (f_2[(n+1)\Delta t], \gamma_0^n, \gamma_1^n, ..., \gamma_{M-1}^n, \gamma_M^n, f_3[(n+1)\Delta t])^T.$$

As mentioned in the following section, the system's solution can be obtained at any time level by inserting the initial vector Γ^0. In the next section, we will find the initial vector.

3 Initial Vector

With the help of the initial condition defined in (3) and their derivatives at boundary points as

$$\begin{aligned} u(x,0) &= f_1(x), \\ u_{xx}(r,0) &= \left.\frac{d^2 f_1(x)}{dx^2}\right|_r, \\ u_{xx}(s,0) &= \left.\frac{d^2 f_1(x)}{dx^2}\right|_s, \end{aligned}$$

we can find the initial vector Γ^0. Discretising the above equations and using (16) and (18), we get

$$(\alpha_{i-1}^0 + 4\alpha_i^0 + \alpha_{i+1}^0) = f_1(r+ih), \tag{33}$$

$$\frac{1}{2h^2}(14\alpha_{-1}^{n+1} - 33\alpha_0^{n+1} + 28\alpha_1^{n+1} - 14\alpha_2^{n+1} + 6\alpha_3^{n+1} - \alpha_4^{n+1}) = \left.\frac{d^2 f_1(x)}{dx^2}\right|_r, \tag{34}$$

$$\begin{aligned} \frac{1}{2h^2}(14\alpha_{M+1}^{n+1} - 33\alpha_M^{n+1} + 28\alpha_{M-1}^{n+1} - 14\alpha_{M-2}^{n+1} + 6\alpha_{M-3}^{n+1} - \alpha_{M-4}^{n+1}) \\ = \left.\frac{d^2 f_1(x)}{dx^2}\right|_s. \end{aligned} \tag{35}$$

From the above equations, we will get a matrix of order $(M+3) \times (M+3)$ defined as

$$\Omega^0 C^0 = \Gamma^0, \tag{36}$$

where

$$\Omega^0 = \begin{pmatrix} 14 & -33 & 28 & -14 & 6 & -1 & \cdots & 0 & 0 \\ 1 & 4 & 1 & 0 & 0 & 0 & \cdots & 0 & 0 \\ 0 & 1 & 4 & 1 & 0 & 0 & \cdots & 0 & 0 \\ \vdots & \vdots & \vdots & \vdots & \vdots & \vdots & \ddots & \vdots & \vdots \\ \vdots & \vdots & \vdots & \vdots & \vdots & \vdots & \ddots & \vdots & \vdots \\ 0 & 0 & \cdots & 0 & 0 & 1 & 4 & 1 & 0 \\ 0 & 0 & \cdots & 0 & 0 & 0 & 1 & 4 & 1 \\ 0 & 0 & \cdots & -1 & 6 & -14 & 28 & -33 & 14 \end{pmatrix}$$

and

$$C^0 = (\alpha_{-1}^0, \alpha_0^0, \alpha_1^0, \ldots\ldots, , \alpha_M^0, \alpha_{M+1}^0)^T,$$

$$\Gamma^0 = \left(h^2 \left. \frac{d^2 f_1(x)}{dx^2} \right|_r, f_1(r), f_1(r+h), f_1(r+2h), \ldots\ldots, f_1(s), h^2 \left. \frac{d^2 f_1(x)}{dx^2} \right|_s \right)^T.$$

The solution of the system (36) will provide the initial vector. Using this initial vector, we can get the approximate solution of the proposed model using equation (32) at any time. In the next section, we will discuss the stability of the derived scheme.

4 Stability Analysis

With the help of the Fourier method, we will show the stability of the scheme. A numerical scheme must have bounded absolute error, denoted by $e(x,t) = \|u(x,t) - f(x,t)\|$, to become stable. Let us assume $u^n = \beta$, where β is a local constant [26, 27]. The proposed numerical scheme is given by (20)

$$\begin{aligned} &(\alpha_{i-1}^{n+1} + 4\alpha_i^{n+1} + \alpha_{i+1}^{n+1}) \left(1 - \frac{D\Delta t}{2}(u_{xx})_i^n + \frac{\nu\Delta t}{2}(u_x)_i^n + \frac{\lambda\Delta t}{2} - \lambda\Delta t u_i^n \right) \\ &- \left(\frac{D\Delta t}{4h^2} u_i^n \right) (\alpha_{i-2}^{n+1} + 8\alpha_{i-1}^{n+1} - 18\alpha_i^{n+1} + 8\alpha_{i+1}^{n+1} + \alpha_{i+2}^{n+1}) - \frac{3\Delta t}{h} \\ &\qquad \left(D(u_x)_i^n - \frac{\nu}{2} \right) (\alpha_{i+1}^{n+1} - \alpha_{i-1}^{n+1}) = u_i^n \left(1 - \frac{\lambda\Delta t}{2} \right). \end{aligned}$$

Let us consider that

$$S = \left(1 - \frac{D\Delta t}{2}(u_{xx})_i^n + \frac{\nu\Delta t}{2}(u_x)_i^n + \frac{\lambda\Delta t}{2} - \lambda\Delta t u_i^n \right); \quad P = \left(\frac{D\Delta t}{4h^2} u_i^n \right);$$

$$Q = \frac{3\Delta t}{h}\left(D(u_x)_i^n - \frac{\nu}{2}\right); R = \left(1 - \frac{\lambda \Delta t}{2}\right).$$

Entering these values into the equation above yields

$$S(\alpha_{i-1}^{n+1} + 4\alpha_i^{n+1} + \alpha_{i+1}^{n+1}) - P(\alpha_{i-2}^{n+1} + 8\alpha_{i-1}^{n+1} - 18\alpha_i^{n+1} + 8\alpha_{i+1}^{n+1} + \alpha_{i+2}^{n+1})$$
$$- Q(\alpha_{i+1}^{n+1} - \alpha_{i-1}^{n+1}) = R(\alpha_{i-1}^n + 4\alpha_i^n + \alpha_{i+1}^n). \quad (37)$$

Substituting $\alpha_i^n = Ae^n \exp(ij\phi h)$, where e^n is error in the n^{th} iteration, $j = \sqrt{-1}$, $'A'$ is the amplitude, h is step length and ϕ is mode number in equation (37), we get

$$e^{n+1}[S(e^{-j\phi h} + 4 + e^{j\phi h}) - P(e^{-2j\phi h} + 8e^{-j\phi h} - 18 + 8e^{j\phi h} + e^{2j\phi h}) \quad (38)$$
$$-Q(e^{j\phi h} - e^{-j\phi h})] = e^n[R(e^{-j\phi h} + 4 + e^{j\phi h})],$$

$$e = \frac{R(\cos z + 2)}{S(\cos z + 2) - P(\cos 2z + 8\cos z - 9) - jQ\sin z},$$

where $z = j\phi h$. Let us take $a = R(\cos z + 2), b = S(\cos z + 2) - P(\cos 2z + 8\cos z - 9)$ and $c = Q\sin z$, then

$$e = \frac{a}{b - jc}.$$

For the numerical scheme to be stable, we have

$$|e| \leq 1$$
$$\implies \left|\frac{a}{b - jc}\right| \leq 1$$
$$\implies -1 \leq \frac{a}{\sqrt{b^2 + c^2}} \leq 1$$

In first case,

$$-1 \leq \frac{a}{\sqrt{b^2 + c^2}}$$
$$\implies 1 \leq \frac{a^2}{b^2 + c^2}$$
$$\implies b^2 + c^2 - a^2 \leq 0$$

In second case,

$$\begin{aligned} &\frac{a}{\sqrt{b^2+c^2}} \geq 1 \\ \implies &\frac{a^2}{b^2+c^2} \geq 1 \\ \implies &b^2+c^2-a^2 \geq 0 \end{aligned}$$

From both cases, we get $|b^2+c^2-a^2| \geq 0$.
The optimum value of

$$b^2+c^2-a^2 = \{S(\cos z+2) - P(\cos 2z + 8\cos z - 9)\}^2 + \{Q \sin z\}^2 \\ - \{R(\cos z + 2)\}\}^2.$$

is obtained when $\cos z = 1$.
By putting this, we get

$$b^2+c^2-a^2 = 9(S^2-R^2).$$

Now, putting the values of S and R, we get

$$|b^2+c^2-a^2| = |9\lambda\Delta t(1-\beta)(2-\lambda\Delta t\beta)|,$$

As $9\Delta t(1-\beta)(2-\lambda\Delta t\beta) > 0$, so for $|\lambda| \geq 0$ our proposed numerical scheme is unconditionally stable.

5 Numerical examples

This section applies the derived numerical scheme to three standard numerical problems, specific instances of the nonlinear RADE. (2), along with the appropriate boundary conditions to validate the effectiveness of the numerical scheme. To solve the discretised system, the authors did all the calculations on a Lenovo laptop(11th Gen Intel Core i5,16 GB 2.40GHz) with Mathematica 12. The computational time to perform every operation is approximately 0.05 seconds. An accurate comparison is made between the numerical solutions achieved and the exact solutions, and error is calculated using l^2 and l^∞ norms defined as

$$||u(x,t_n) - f(x,t_n)||_{l^2} = \sqrt{h\sum_{i=0}^{M} |u(x_i,t_n) - f(x_i,t_n)|^2},$$

$$||u(x,t_n) - f(x,t_n)||_{l^\infty} = \max_{0\leq i\leq M} |u(x_i,t_n) - f(x_i,t_n)|,$$

where the partial differential equation's precise and numerical solutions are denoted by the symbols $u(x,t)$ and $f(x,t)$, respectively.

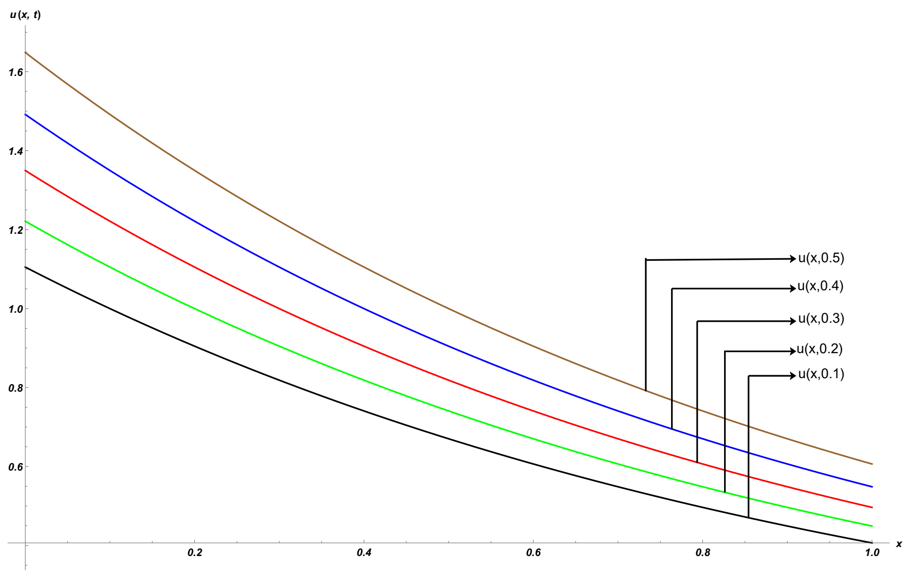

Figure 1: Plot of the solution for Example 1

5.1 Example 1

Let us consider $D = 1$, $\nu = -1$ and $\lambda = -1$, which reduces the model (2) as

$$\frac{\partial u}{\partial t} = \frac{\partial}{\partial x}\left(u\frac{\partial u}{\partial x}\right) + u\frac{\partial u}{\partial x} + u(1-u), \tag{39}$$

whose exact solution is $u(x,t) = \exp(t-x)$[28]. After solving the problem (39) numerically for $h = 0.05$ and $\Delta t = 0.01$, the obtained results are shown through Fig.1. Table 2 displays the errors for different values of x and t that were found when comparing the exact findings with the numerical solution. The suggested numerical approach is quite accurate, as indicated by the table.

5.2 Example 2

Considering the mathematical model (2) without reaction term i.e., for $D = 1, \nu = 1$ and $\lambda = 0$, which is reduced to

$$\frac{\partial u}{\partial t} = \frac{\partial}{\partial x}\left(u\frac{\partial u}{\partial x}\right) - u\frac{\partial u}{\partial x}, \tag{40}$$

Table 2: Variations of errors for Example 1 at different times

t(sec)	l^2 error	l^∞ error
0.1	7.17588×10^{-3}	1.01079×10^{-2}
0.2	9.69107×10^{-3}	1.40418×10^{-2}
0.3	9.18371×10^{-3}	1.35965×10^{-2}
0.4	6.89232×10^{-3}	1.09177×10^{-2}
0.5	4.02909×10^{-3}	6.71902×10^{-3}

Table 3: Variations of errors for Example 2 at different times

t(sec)	l^2 error	l^∞ error
0.25	2.05374×10^{-2}	2.80308×10^{-2}
0.50	1.53846×10^{-2}	2.10831×10^{-2}
0.75	1.17253×10^{-2}	1.60885×10^{-2}
1.00	0.900954×10^{-2}	1.23741×10^{-2}

having exact solution $u(x,t) = \frac{\ln(t+1)+x+2}{t+1}$ [21] for appropriate initial and boundary conditions.
The numerical solution is obtained by taking $h = 0.05$ and $\Delta t = 0.05$. The obtained errors are shown in Table 3 for different time levels, which demonstrate the excellent performance of the suggested numerical technique even for extremely short temporal and spatial discretisations.

5.3 Example 3

Considering another set of parameters $D = 1, \nu = 0$ and $\lambda = -1$, for which our proposed model (2) is reduced to

$$\frac{\partial u}{\partial t} = \frac{\partial}{\partial x}\left(u\frac{\partial u}{\partial x}\right) + u(1-u), \tag{41}$$

having the exact solution given by

$$u(x,t) = \frac{1}{4}\left[1 - \tanh\left\{\frac{1}{2\sqrt{6}}\left(x - \frac{5t}{\sqrt{6}}\right)\right\}\right]^2 \tag{42}$$

for appropriate initial and boundary conditions. The diffusion equation is numerically solved by applying the suggested numerical scheme for $h = 0.05$ and $\Delta t = 0.05$. The maximum absolute and root mean square errors are

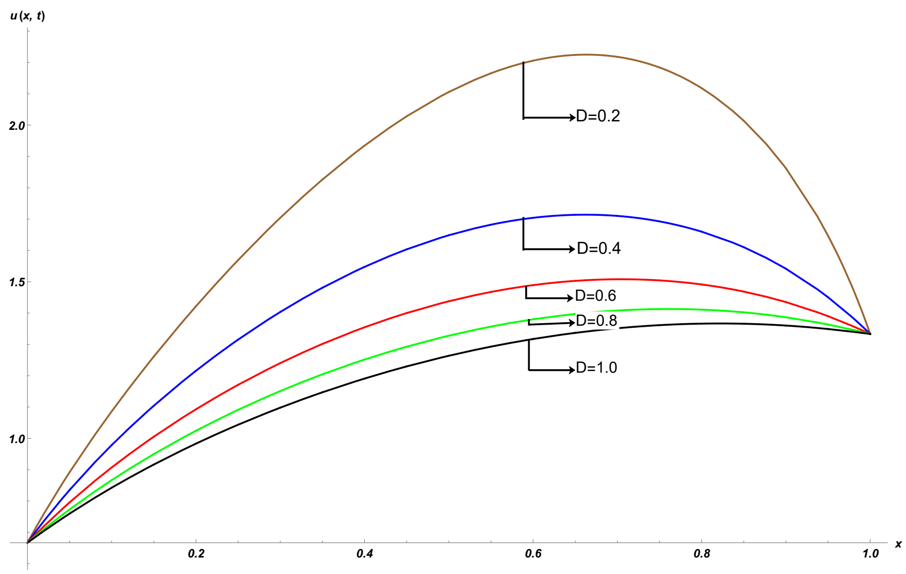

Figure 2: Effect on solute profile with the variation in D at $t = 0.5sec$ for $\nu = 0.6$ and $\lambda = 1$

obtained using l^2 and l^∞ norms, respectively. Table 4 shows that the proposed numerical scheme performs well.

6 Solution of the proposed nonlinear RADE model

Once the suggested numerical approach has been verified on three distinct examples of our pertinent mathematical model, (2), the authors have applied it to the model (2) under the following prescribed initial and boundary conditions as given by

$$u(x, 0) = x + 1, \tag{43}$$

$$u(0, t) = \frac{1}{1 + t}, \tag{44}$$

$$u(1, t) = \frac{2}{1 + t}. \tag{45}$$

The numerical solution of the nonlinear RADE (2) is obtained using the proposed numerical scheme through the discretisation with $h = 0.05$ and

Table 4: Variations of errors for Example 3 at different times

t(sec)	l^2 error	l^∞ error
0.1	1.35658×10^{-3}	1.90915×10^{-3}
0.2	1.43863×10^{-3}	2.09177×10^{-3}
0.3	6.46713×10^{-4}	1.04007×10^{-3}
0.4	6.57265×10^{-4}	9.54313×10^{-4}
0.5	1.74904×10^{-3}	2.35696×10^{-3}

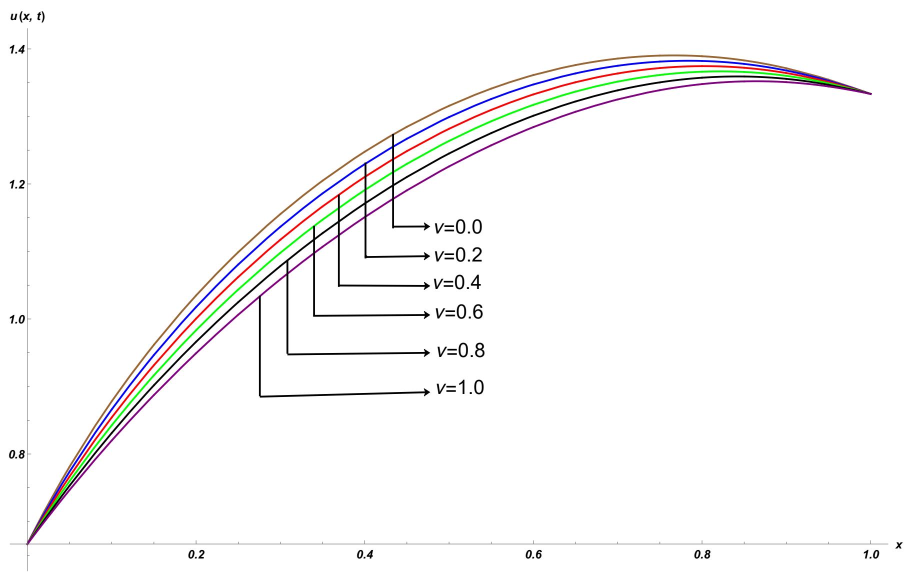

Figure 3: Effect on solute profile with the variation in ν at $t = 0.5sec$ for $D = 1$ and $\lambda = 1$

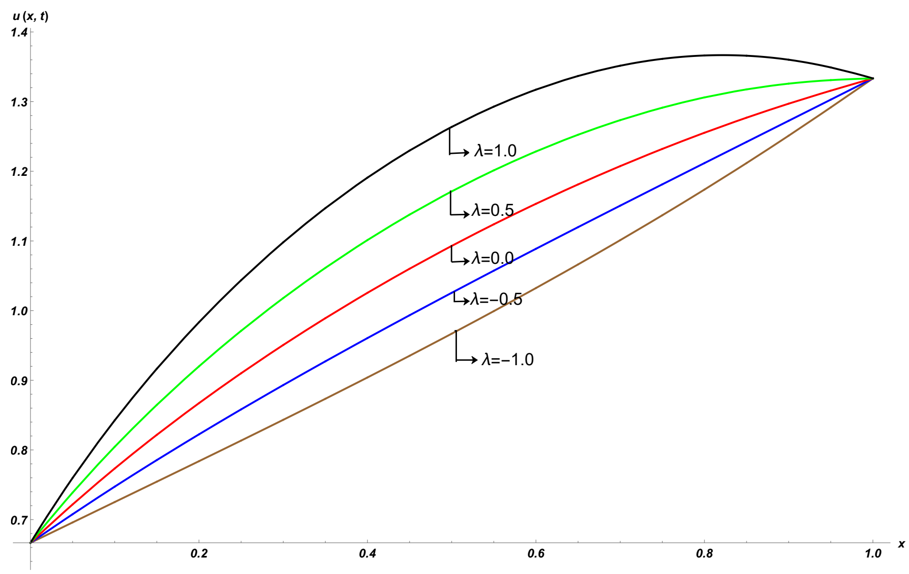

Figure 4: Effect on solute profile with the variation in λ at $t = 0.5sec$ for $D = 1$ and $\nu = 0.6$

$\Delta t = 0.05$. Fig.2 shows the effect of variation in diffusion coefficient D in the presence of advection and reaction coefficients. It shows that an increase in the diffusion coefficient decreases the solute profile. Fig.3 shows the decrease in the solute profile with an increase in the nonlinear advection coefficient when diffusion and reaction coefficients are one. While taking diffusion and advection coefficients 1 and 0.6, respectively, the effect of variation in reaction coefficient is shown in Fig.4. This figure shows the decline in the solute profile as the reaction coefficient increases. These figures clearly show the effect of nonlinearity in the proposed model's three main components, viz. diffusion, advection and reaction on the solute profile.

7 Conclusion

An innovative numerical approach to solve the nonlinear RADE with given initial and boundary conditions is presented in this study. The scheme is based on the characteristics of the cubic B-spline. Furthermore, the numerical technique is demonstrated to be unconditionally convergent. Using conventional but relevant data, the scheme's application has been shown for various grid sizes and values of D, ν and λ. A comparison between the obtained numerical results and the exact results through error analysis leads to the conclusion that the suggested approach works effectively and the computed results match the exact results. The key contributions of the present study are the presentation of the effectiveness and accuracy of the proposed approach and the observation of the solute profile with the changes in the reaction, advection, and diffusion coefficients.

Acknowledgements

The authors would like to thank the reviewers for their constructive comments and suggestions to improve the quality of the revised article. The third author acknowledges the project grant provided by the Board of Research in Nuclear Sciences (BRNS), BARC, Government of India (sanction no. 58/14/07/2022-BRNS/37041).

Conflict of interest

The authors declare that they don't have any conflict of interest.

References

[1] Bear, J. (2013). Dynamics of fluids in porous media. *Courier Corporation*.

[2] Dagan, G. (2012). Flow and transport in porous formations. *Springer Science & Business Media*.

[3] De Ghislain, M. (1986). Quantitative hydrogeology; groundwater hydrology for engineers.

[4] Durlofsky, L., & Brady, J. F. (1987). Analysis of the Brinkman equation as a model for flow in porous media. *Physics of Fluids*, 30(11), 3329.

[5] Richard, L. A. (1931). Capillary conduction of liquids through porous mediums. *Physics*, 1(5), 318-333.

[6] Lucas, T. R. (1974). Error bounds for interpolating cubic splines under various end conditions. *SIAM Journal on Numerical Analysis*, 11(3), 569-584.

[7] Fisher, R. A. (1937). The wave of advance of advantageous genes. *Annals of eugenics*, 7(4), 355-369.

[8] Kenkre, V. M. (2004). Results from variants of the Fisher equation in the study of epidemics and bacteria. *Physica A: Statistical Mechanics and its Applications*, 342(1-2), 242-248.

[9] Tyson, J. J., & Fife, P. C. (1980). Target patterns in a realistic model of the BelousovZhabotinskii reaction. *The Journal of Chemical Physics*, 73(5), 2224-2237.

[10] Bramson, M. D. (1978). Maximal displacement of branching Brownian motion. *Communications on Pure and Applied Mathematics*, 31(5), 531-581.

[11] De Loubens, R., & Ramakrishnan, T. (2011). Asymptotic solution of a nonlinear advection-diffusion equation. *Quarterly of applied mathematics*, 69(2), 389-401.

[12] De Loubens, R., & Ramakrishnan, T. S. (2011). Analysis and computation of gravity-induced migration in porous media. *Journal of fluid mechanics*, 675, 60-86.

[13] Polyanin, A. D., & Zhurov, A. I. (2014). The functional constraints method: Application to non-linear delay reactiondiffusion equations with varying transfer coefficients. *International Journal of Non-Linear Mechanics*, 67, 267-277.

[14] Sherratt, J. A., & Marchant, B. P. (1996). Nonsharp travelling wave fronts in the Fisher equation with degenerate nonlinear diffusion. *Applied Mathematics Letters*, 9(5), 33-38.

[15] Lu, J., Yu-Cui, G., & Shu-Jiang, X. (2007). Some new exact solutions to the BurgersFisher equation and generalized BurgersFisher equation. *Chinese Physics*, 16(9), 2514.

[16] Mittal, R. C., & Arora, G. (2010). Efficient numerical solution of Fisher's equation by using B-spline method. *International Journal of Computer Mathematics*, 87(13), 3039-3051.

[17] Jaiswal, S., Chopra, M., & Das, S. (2019). Numerical solution of nonlinear partial differential equation for porous media using operational matrices. *Mathematics and Computers in Simulation*, 160, 138-154.

[18] Dwivedi, K. D., & Das, S. (2019). Numerical solution of the nonlinear diffusion equation by using non-standard/standard finite difference and Fibonacci collocation methods. *The European Physical Journal Plus*, 134(12), 608.

[19] Berryman, J. G., & Holland, C. J. (1978). Nonlinear diffusion problem arising in plasma physics. *Physical Review Letters*, 40(26), 1720.

[20] Rohila, R., & Mittal, R. (2018). Numerical study of reaction diffusion Fishers equation by fourth order cubic B-spline collocation method. *Mathematical Sciences*, 12, 79-89.

[21] Pudasaini, S. P., Ghosh Hajra, S., Kandel, S., & Khattri, K. B. (2018). Analytical solutions to a nonlinear diffusionadvection equation. *Zeitschrift fr angewandte Mathematik und Physik*, 69, 1-20.

[22] Singh, A., Dahiya, S., & Singh, S. P. (2020). A fourth-order B-spline collocation method for nonlinear BurgersFisher equation. *Mathematical Sciences*, 14, 75-85.

[23] Mittal, R. C., & Jain, R. K. (2013). Numerical solutions of nonlinear Fisher's reactiondiffusion equation with modified cubic B-spline collocation method. *Mathematical Sciences*, 7(1), 12.

[24] Kumar, R., & Arora, S. (2022). solution of fisher Kolmogorov Petrovsky equation driven via Haar scale-3 wavelet collocation method. *International Journal of Mathematical, Engineering and Management Sciences*, 7(5), 717-729.

[25] Ahmad, Z., & Kothyari, U. C. (2001). Time-line cubic spline interpolation scheme for solution of advection equation. *Computers & fluids*, 30(6), 737-752.

[26] Siddiqi, S. S., & Arshed, S. (2014). Quintic B-spline for the numerical solution of the good Boussinesq equation. *Journal of the Egyptian Mathematical Society*, 22(2), 209-213.

[27] Wasim, I., Abbas, M., & Amin, M. (2018). Hybrid BSpline Collocation Method for Solving the Generalized BurgersFisher and BurgersHuxley Equations. *Mathematical Problems in Engineering*, 2018(1), 6143934.

[28] Cherniha, R., Serov, M., & Rassokha, I. (2008). Lie symmetries and form-preserving transformations of reactiondiffusionconvection equations. *Journal of mathematical analysis and applications*, 342(2), 1363-1379.

[29] Buckingham, E. (1907). Studies on the movement of soil moisture. *US Dept. Agic. Bur. Soils Bull.*, 38.

[30] Rogers, J. R., & Fredrich, A. J. (Eds.). (2001, October). International Engineering History and Heritage: Improving Bridges to ASCE's 150th Anniversary. *American Society of Civil Engineers.*

[31] Kovarik, K. (2012). Numerical models in groundwater pollution. *Springer Science & Business Media.*

Eduard-Marius Craciun,
Faculty of Mechanical, Industrial and Maritime Engineering,
Ovidius University of Constanta Bd. Mamaia 124,
900527 Constanta, Romania.
Academy of Romanian Scientists,
3, Ilfov str.,
050044, Bucharest, Romania.
Email: mcraciun@univ-ovidius.ro

Shubham Kumar Tiwari,
Department of Mathematical Sciences,
Indian Institute of Technology (BHU),
Varanasi-221005, India.
Email: shubhamkrtiwari.rs.mat18@itbhu.ac.in

Subir Das,
Department of Mathematical Sciences,
Indian Institute of Technology (BHU),
Varanasi-221005, India.
Email: sdas.apm@iitbhu.ac.in